

# Effect of Casting Conditions on Layer Porosity and Entrained Bubbles in Gravity-filled TiAlNb Castings

Gong Ziqi, Chai Lihua, Zhou Feng, Chen Ziyong, Nie Zuoren

Beijing University of Technology, Beijing 100124, China

**Abstract:** Gravity-pouring of a TiAlNb alloy from an induction skull melting (ISM) furnace into a ceramic shell mould was carried out. The microstructure and gas defects were examined by scanning electron microscopy (SEM), energy-dispersive X-ray (EDX) and X-ray photoelectron spectroscopy (XPS) analysis. Results show that the oxide films exist in the bubbles and porosity, and act as defects' heterogeneous nucleation sites. The bubbles consist of entrained and precipitable ones, while the porosity consist of layer and centerline ones. The diameter of casting bars, mould temperature and the partial pressure of argon influence the formation of gas defects.

**Key words:** titanium aluminide based alloys; casting; microstructure; defects

TiAl alloys have been considered as candidate materials in the fields of aerospace and automobile in 21st century, especially served in the temperature range of 833~1073 K<sup>[1-3]</sup>. During the past two decades, substantial improvements have been made in material properties, processing techniques and design methodologies. However, some problems haven't been solved completely, such as room temperature brittleness, poor workability and deformability, no enough creep and oxidation resistance above 1073 K, reverse relationship between tensile strength and ductility & creep resistance, and no enough microstructure stability at elevated temperature, which are influenced greatly by compositions, forming methods and heat treatments. The investment casting is usually considered to be the most appropriate and lower cost shaping method to solve the problems of low ductility and poor workability for TiAl alloys<sup>[4-8]</sup>.

TiAl castings are usually produced by induction skull melting (ISM) in a bottom-pouring water-cooled copper crucible operated under vacuum or inert gas atmosphere to prevent melt from contamination<sup>[9-13]</sup>. ISM can provide a high quality melt with very low interstitial elements, such as oxygen, nitrogen and hydrogen, but it has a very limited

superheat. For example, ISM rarely provides a superheat beyond 293 K. Consequently, it is a common practice to "dump pour" the liquid metal from an ISM furnace into a mould. The uncontrolled chaotic flow of the liquid metal into the mould generates severe surface break-up and entrains bubbles into the flowing metal, with the risk of leaving surface films and bubbles trapped inside the final castings<sup>[14-17]</sup>. Simultaneously, oxide films may form. The films are commonly thought to root in soluble oxygen in molten TiAl alloys or come from the ceramic mould. However, TiAl alloy is usually melted under vacuum or inert gas atmosphere and the ceramic mould is also baked at elevated temperature. It is very crucial for the properties of TiAlNb alloys whether or not films exist in it. Porosity defects commonly emerged in gravity-pouring castings, which badly influence the ductility and toughness of the castings. Some researchers show that argon is an important factor that influences the compactness of  $\gamma$ -TiAl<sup>[18-22]</sup>.

In the present paper, a series of trials were carried out to investigate how the principal casting parameters (section size, mould temperature, melting/casting atmosphere) affect the occurrence of entrained bubbles and layer porosity in

Received date: October 25, 2015

Foundation item: EU and ESA through the IMPRESS Integrated Project-Intermetallic Materials Processing in Relation to Earth and Space Solidification (NMP3-CT-2004-500635); National Natural Science Foundation of China (51301005)

Corresponding author: Chen Ziyong, Ph. D., Professor, College of Materials Science and Engineering, Beijing University of Technology, Beijing 100124, P. R. China, Tel: 0086-10-67392280, E-mail: czy@bjut.edu.cn

Copyright © 2016, Northwest Institute for Nonferrous Metal Research. Published by Elsevier BV. All rights reserved.

gravity-casting Ti-46Al-8Nb casting. The reasons for the formation of the defects were also analyzed.

## 1 Experiment

An ISM furnace equipped with a water-cooled copper crucible was used in this research and has a capacity to melt 5 kg of TiAl alloys in vacuum or in argon atmosphere. A stepped power-time sequence was adopted in many previous melts. Power was applied to the ISM coil to melt the 4.5 kg charge of Ti-46Al-8Nb alloy (a piece cut from a plasma melted billet). The molten metal was gravity-poured into the mould. Each mould was placed inside a graphite mould heating furnace inside the vacuum chamber housed in the ISM furnace. The chamber was evacuated to 5 Pa and vacuum leak was checked. The moulds were heated to either 773 K or 1273 K and baked at this temperature for 1 h. Some melts were carried out in vacuum, and for others, the vacuum chamber was back-filled with argon at a partial pressure of either  $2 \times 10^4$  Pa or  $8 \times 10^4$  Pa. Each melt in the experimental matrix (two mould temperatures and three different melting atmospheres) was carried out in duplicate.

The test castings contained 9 bars with 200 mm in length, and the diameters are as follows: three pairs of bars with the diameters of 10, 15 and 20 mm, one of 30 mm, and two bars which tapered from 28 mm to 13 mm. The mould consisted of a conical pouring basin and a disc-shaped feeder to which the test bars were attached. A series of moulds were made using the ceramic shelling process (dewaxed, fired at 1273 K, then cooled to room temperature, inspected and stored prior to use).

The samples for metallographic examination were cut from the TiAl bars using electrical discharge machining. They were abraded by the initial grinding with MD-Piano 220 disc + water for 1 min, the second grinding with MD-Largo disc + DP-Susp.P. 9  $\mu\text{m}$  & DP-Blue for 6 min, and the final polishing with MD-Chen disc + OP-S. 0.04  $\mu\text{m}$  for 4 min. The electro-polishing specimens for the backscattered electron (BSE) detection image and EDX were done with a solution of methanol & 2-Butoxyethanol

+ perchloric acid under 40 kV + 15 s + room temperature. The LEO 32 program was applied for SEM analysis, with an acceleration voltage of 15 kV. The Noran Instruments Vantage -DI X-ray microanalysis system was used to investigate the microanalysis for the porosities and entrained bubbles of castings. All specimens were sectioned along the axis, and group control experiment sampling location were the same.

## 2 Results and Discussion

### 2.1 Compositions of castings

The actual compositions of the casting bars are present in Table 1. The corresponding nominal compositions are all Ti-46Al-8Nb (at%), while the actual compositions were 44.95 at%~46.92 at% Al, and 7.63 at%~8.31 at% Nb. Several bars did not conform to specification. Although undesirable, it would not affect the validity of any observation and analysis of the gas defects. The content of oxygen is about 0.05wt%.

### 2.2 Effect of casting parameters on soundness of castings

The radiographs of bars with diameter of 20 mm cast under different conditions are shown in Fig.1.

All the bars contain layer porosity and some bars contain bubbles, even the bars cast under vacuum contain bubbles. When a mould temperature of 773 K was adopted, casting in vacuum result in more entrained bubbles (594 and 595) than melting carried out under  $2 \times 10^4$  Pa of argon (583 and 587). The higher mould temperature (590 and 591) and higher partial pressure (588 and 589) tend to result in fewer bubble defects. To evaluate the effect of bar size, bars with diameter of 10, 15, and 30 mm were also conducted. With the diameter increasing, there are generally fewer bubbles, possibly because the molten metal solidifies more slowly in the larger diameter bars and gives time for bubbles to coalesce and float out of the bars. It is noticed that all bars contain considerable porosities, particularly those cast under vacuum and poured into a mould at 1273 K.

**Table 1** Compositions analysis of the casting bars under different atmospheres and different mould temperatures

Bar No.	Atmosphere	Mould temperature/K	Ti		Al		Nb		O	
			wt%	at%	wt%	at%	wt%	at%	wt%	at%
594	Vacuum	773	52.95	46.05	29.9	46.15	17.1	7.67	0.05	0.130
595			53.26	46.84	28.8	44.95	17.9	8.11	0.04	0.105
592		1273	53.35	46.73	29.1	45.24	17.5	7.90	0.05	0.131
593			53.26	46.63	29.2	45.37	17.5	7.90	0.04	0.105
583	$2 \times 10^4$ Pa (Ar)	773	51.64	44.91	30.4	46.92	17.9	8.02	0.06	0.156
587			53.35	46.63	29.3	45.45	17.3	7.79	0.05	0.131
581		1273	51.94	45.51	29.6	46.03	18.4	8.31	0.06	0.157
582			53.24	46.34	29.7	45.88	17.0	7.63	0.06	0.156
588	$8 \times 10^4$ Pa (Ar)	773	53.05	46.17	29.8	46.03	17.1	7.67	0.05	0.130
589			52.65	45.85	29.9	46.21	17.4	7.81	0.05	0.130
590		1273	52.85	46.29	29.3	45.54	17.8	8.04	0.05	0.131
591			52.45	45.82	29.7	46.04	17.8	8.01	0.05	0.131

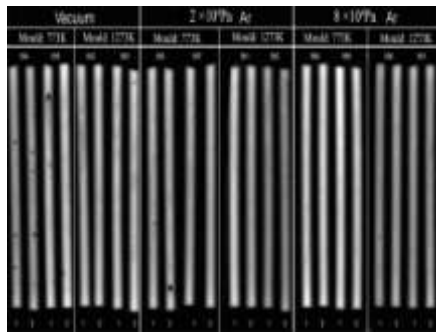


Fig.1 Radiographs of 20 mm diameter bars cast under different casting conditions

The radiographs of tapered bars cast under vacuum at two different mould temperatures of 773 and 1273 K are presented in Fig.2a. When a mould temperature of 773 K is adopted, there are fewer bubbles compared with a mould temperature of 1273 K and no sign of layer porosity is manifested. There are occasional bubbles when the tapered bars cast under  $2 \times 10^4$  Pa of argon, but no sign of layer porosity emerges, as shown in Fig.2b. When increasing the partial pressure of argon to  $8 \times 10^4$  Pa, it seems to result in a further reduction of entrained bubbles, as shown in Fig.2c. In view of the apparent absence of layer porosity in tapered bars, one tapered bar 582 ( $2 \times 10^4$  Pa argon, mould temperature 1273 K) was sectioned longitudinally. Although no layer porosity is visible in the radiograph, there are relatively small amount of porosities visible on a polished longitudinal section, as shown in Fig.2d.

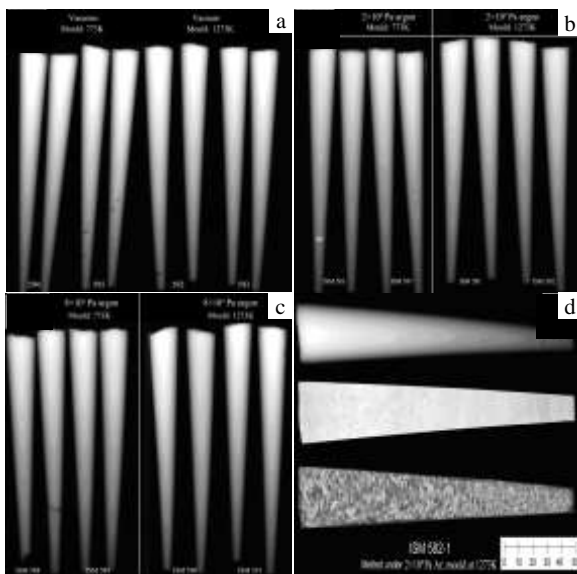


Fig.2 Radiographs of tapered bars cast at two mould temperatures: (a) under vacuum, (b)  $2 \times 10^4$  Pa argon, (c)  $8 \times 10^4$  Pa argon, and (d) tapered bar 582 cast under  $2 \times 10^4$  Pa argon at mould temperature of 1273 K

### 2.3 Defects

#### 2.3.1 Bubbles and porosities

The morphologies of the bubbles and porosities in bars cast under different casting conditions are given in Fig.3. Under vacuum and the mould temperature of 773 K, large bubbles with diameter of about 1.6 mm appear near the surface of the bar, while small shrinkage porosities with size of about  $500 \mu\text{m}$  occur near the center of the bar (Fig.3a and 3b). Fig.3c and 3d present the defects of the bar cast under vacuum and the mould temperature of 1273 K, showing the size of the bubbles and porosities is reduced, but the amount

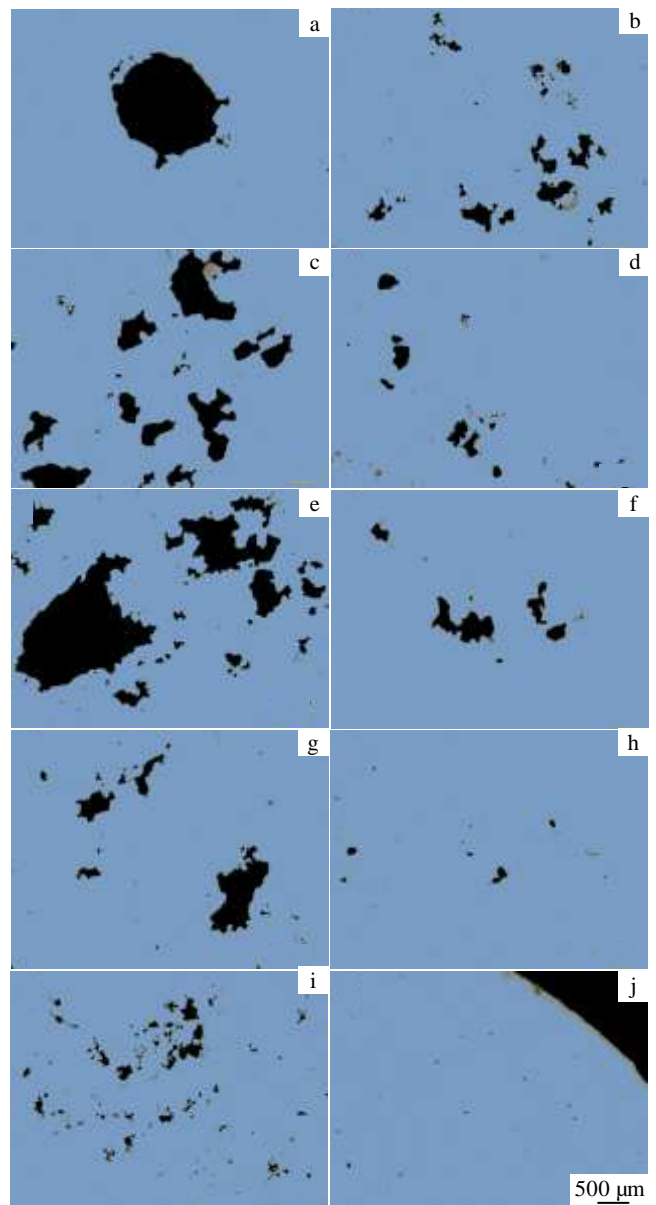


Fig.3 Bubbles and porosities of the bars cast under different atmospheres and different mould temperatures: (a, b) 594 bar vacuum + 773 K, (c, d) 592 bar vacuum + 1273 K, (e, f) 583 bar  $2 \times 10^4$  Pa argon + 773 K, (g, h) 582 bar  $2 \times 10^4$  Pa argon + 1273 K, and (i, j) 590 bar  $8 \times 10^4$  Pa argon + 1273 K

of them is increased as compared with the bar with lower mould temperature of 773 K. When the casting is under  $2 \times 10^4$  Pa argon and mould temperature 773 K, the large bubbles still appear, but the amount of bubbles and porosities is obviously reduced (Fig.3e, 3f and Fig.1). When increasing the mould temperature to 1273 K at the same  $2 \times 10^4$  Pa argon pressure, the size and amount of bubbles and porosities are further decreased (Fig.3g, 3h) compared with Fig.3e and 3f. When the casting condition was  $8 \times 10^4$  Pa argon and the mould temperature of 1273 K, the larger bubbles disappear and some large porosities appear (Fig.3i and 3j).

### 2.3.2 Microstructure and oxide films

The microstructure of 594 bar cast under vacuum and the mould temperature of 773 K is given in Fig.4. It consists of

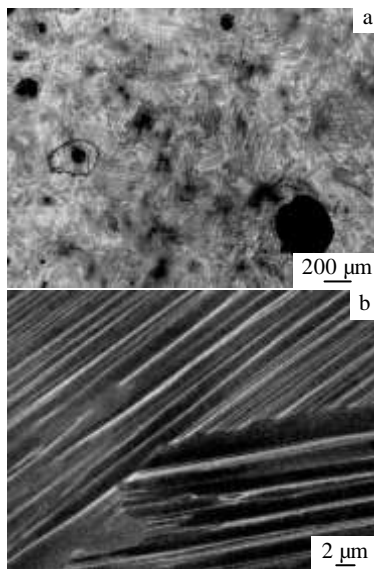


Fig.4 Microstructures of 594 bar cast under vacuum at mould temperature of 773 K

lamellar structure of  $\gamma$ -TiAl and  $\alpha_2$ -Ti<sub>3</sub>Al (Fig.4b). Some bubbles (parts of them exhibit fish-eye morphology) and porosities (Fig.4a) exist in the local area. From surface EDX analysis in Fig.5, the distribution of niobium is uneven, white wing strip-lines are exhibited in Nb-rich areas in the colonies of lamellar structure. The EDX analysis of the large shrinkage porosities in the microstructure of 594 bar indicates that the content of oxygen in or near the hole is higher than that in the matrix (point 11), but it is reverse for niobium, as shown in Fig.6a and Table 2. The composition analysis of a small bubble of 594 bar is given in Fig.6b and Table 3. The oxide films obviously exist in the bubble, and they are mainly Al<sub>2</sub>O<sub>3</sub> and TiO<sub>2</sub> from the spectra. Impurities exist in some small porosities (Fig.6c), which should be Y<sub>2</sub>O<sub>3</sub> particles with bright color, as shown in Table 4.

For 590 bar cast under  $8 \times 10^4$  Pa argon and mould temperature of 1273 K, the microstructure is also lamellar, but the size of the gas defect is obviously reduced, as shown in Fig.7. There is larger content of oxygen in the bubbles and porosities than that in the matrix, as shown in Fig.6d, 6e and Table 5 and Table 6. It illustrates that Al<sub>2</sub>O<sub>3</sub> and TiO<sub>2</sub> exist in the gas defects.

In order to further prove oxides in the gas defects, the XPS composition analysis was employed, as shown in Fig.8 and Fig.9. Fig.8a is the whole surface analysis of 594 bar cast under vacuum and mould temperature of 773 K. Besides Ti, Al, Nb, and a large amount of oxygen is proved to exist, which is the headspring of oxides formation. Fig.8b, 8c, 8d and Fig.9 are the quantity composition analysis inside the gas defects of 594 bar (vacuum, mould temperature of 773 K) and 590 bar ( $8 \times 10^4$  Pa argon, mould temperature of 1273 K), respectively. It is proved that oxide films inside gas defects mainly consist of Al<sub>2</sub>O<sub>3</sub>, TiO<sub>2</sub> and little amount of Nb<sub>2</sub>O<sub>5</sub>.

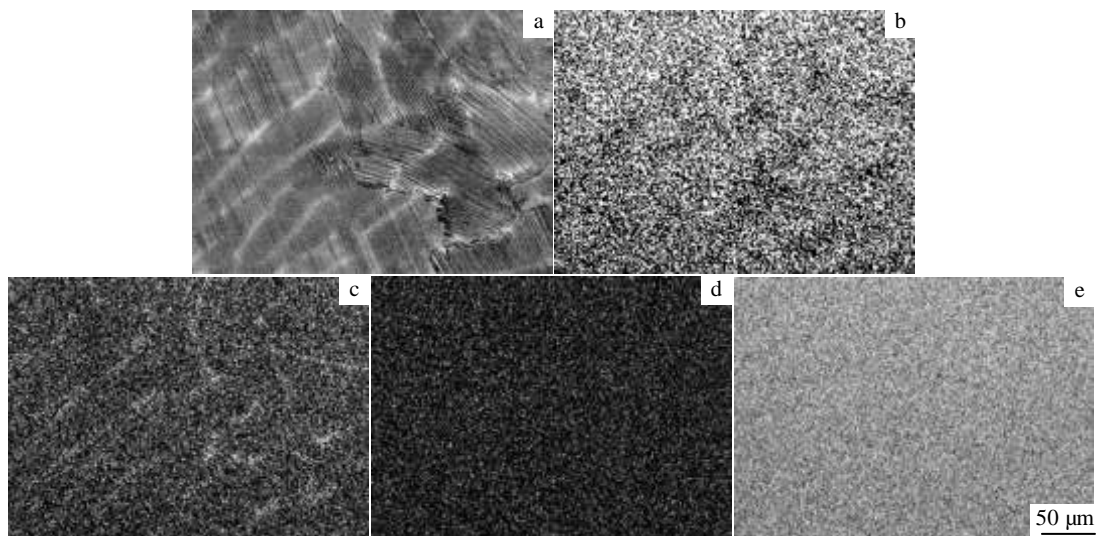


Fig.5 SEM microstructure (a) and EDX area analysis of Al (b), Nb (c), O (d), and Ti (e) elements for 594 bar cast under vacuum and mould temperature of 773 K

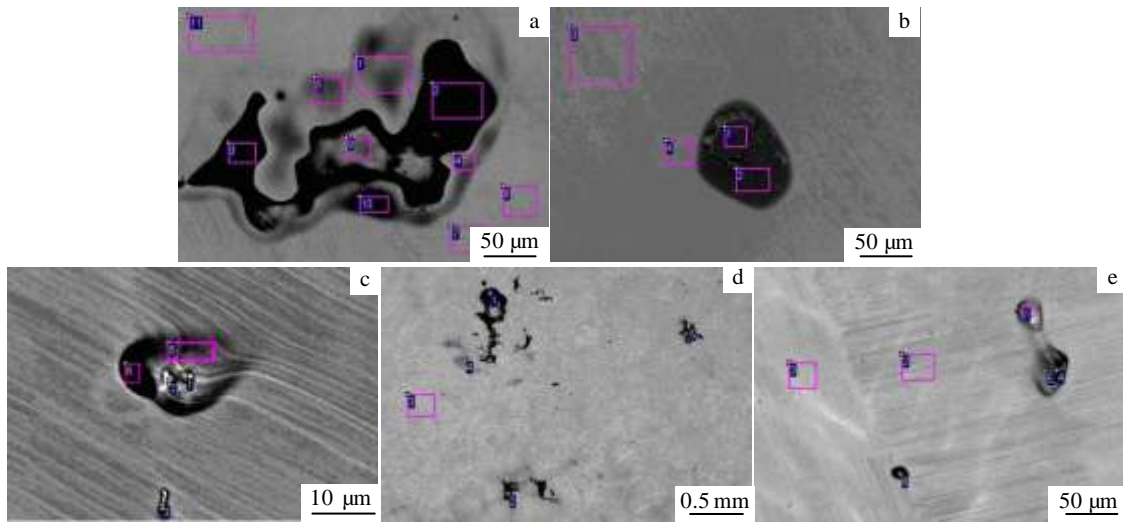


Fig.6 SEM images and EDX point analysis for defects of the bars: (a) the large shrinkage porosities, (b) small bubble, and (c) small porosities of 594 bar cast under vacuum at mould temperature of 773 K; (d, e) EDX point analysis of 590 bar cast under  $8 \times 10^4$  Pa argon at mould temperature of 1273 K

Table 2 EDX point analysis of the large shrinkage porosities of the 594 bar cast under vacuum at mould temperature of 773 K corresponding to Fig.6a (at%)

Point	O	Al	Ti	Nb
1	28.99	32.88	32.93	5.20
2	28.53	33.06	33.13	5.28
3	27.97	33.30	33.38	5.35
4	27.69	33.44	33.57	5.31
5	27.21	33.62	33.82	5.34
6	27.01	33.76	33.80	5.43
7	25.85	34.15	34.55	5.45
9	26.71	33.85	34.07	5.37
10	25.66	34.40	34.40	5.54
11	-	46.25	46.00	7.75

Table 3 EDX point analysis of the small bubbles of the 594 bar cast under vacuum at mould temperature of 773 K corresponding to Fig.6b (at%)

Point	O	Al	Ti	Nb
1	68.49	15.61	13.90	2.00
2	76.11	12.36	10.00	1.52
3	-	46.37	45.93	7.71
4	-	47.58	45.80	6.62

Table 4 EDX point analysis of the small porosities of 594 bar cast under vacuum at mould temperature of 773 K corresponding to Fig.6c (at%)

Point	O	Al	Ti	Y	Nb
1	44.69	12.61	16.28	26.42	0.00
2	44.84	21.17	19.42	12.67	1.91
3	34.66	26.23	26.75	8.82	3.55
5	-	17.85	78.68	-	3.48
6	-	10.76	87.45	-	1.79

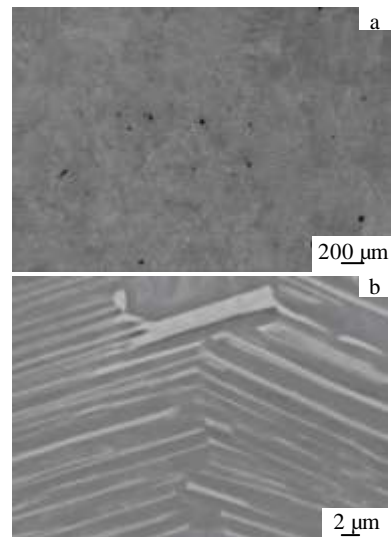


Fig.7 Microstructures of 590 bar cast under  $8 \times 10^4$  Pa argon at mould temperature of 1273 K

## 2.4 Discussion

The above experiments prove that there are large amount of oxygen in the testing bars cast under vacuum or argon atmosphere. The reason is that the oxygen comes from the melting process or from the mould when filled with molten metal. The oxygen forms the oxides such as  $Al_2O_3$ ,  $TiO_2$  and  $Nb_2O_5$ . These oxides will be nucleus for bubbles and some porosities. When liquid metal is filled into mould with sufficient turbulence and temperature, the entrained bubbles with oxide films will be formed.

Due to large aspect ratio of the testing bar, there is not enough temperature gradient along the longitudinal direction during solidification. The shrinkage porosity usually forms



Large amount of bubbles and porosities are formed in colony of lamellar structure, which is the interdendritic area during solidification, as shown in Fig.4 and Fig.7.

### 3 Conclusions

1) Either vacuum or argon atmosphere, the oxide films exist in the bubbles and porosities. The oxide films act as heterogeneous nucleation sites, resulting in the formation of centerline and layer porosity in Ti-Al-Nb castings. The bubbles are precipitable from the melt or entrained from protecting argon or outgas from the mould.

2) As the diameter of casting bars and the mould temperature increases, the gas defects will be reduced. Using tapered casting bars, the gas defects are reduced obviously. Increasing argon partial pressure helps to reduce the bubbles and porosities.

3) The bubbles are located near the columnar surface, and the porosities are mainly located in the centerline of bars, or little near surface, namely, layer porosity. The bubbles and porosities are all located in colony of lamellar structure or interdendritic area during solidification.

**Acknowledgement:** This paper got the H. J. Fecht's help, who is a professor. D. R. of institute of micro and nano materials of Ulm university, Germany greatly appreciated.

### References

- 1 Cao G H, Shen G J, Liu J M et al. *Scripta Materialia*[J], 2003, 49: 797
- 2 Yang Huimin, Su Yanqing, Luo Liangshun et al. *Rare Metal Materials and Engineering*[J], 2011, 40(1): 1 (in Chinese)
- 3 Cheng Liang, Chang Hui, Tang Bin et al. *Rare Metal Materials and Engineering*[J], 2014, 43(1): 36
- 4 Schillingera W, Clemens H. *Intermetallics*[J], 2002, 10: 459
- 5 Jin Y G, Wang J N, Yang J et al. *Scripta Materialia*[J], 2004, 51: 113
- 6 Yang Fei, Kong Fantao, Chen Yuyong et al. *Rare Metal Materials and Engineering*[J], 2011, 40(7): 1505 (in Chinese)
- 7 Chen Y Y, Yang F, Kong F T et al. *Journal of Rare Earth*[J], 2011, 29: 114
- 8 Perez M, Madariaga I, Ostolaza K et al. *Scripta Materialia*[J], 2005, 53: 1141
- 9 Wang Zhe, Cao Rui, Chen Jianhong et al. *Rare Metal Materials and Engineering*[J], 2014, 43(2): 540
- 10 Gong Ziqi, Chen Ziyong, Chai Lihua et al. *Acta Metallurgica Sinica*[J], 2013, 49: 1369 (in Chinese)
- 11 Negrinia F, Fabbria M, Zuccarinia M et al. *Energy Conversion and Management*[J], 2000, 41: 1687
- 12 Bojarevics V, Pericleous K, Cross M. *Metallurgical and Materials Transactions B*[J], 2000, 31: 179
- 13 Su Y Q, Guo J J, Liu G Z et al. *Materials Science and Technology*[J], 2001, 17: 1434
- 14 Moritaa A, Fukuib H, Tadanao H et al. *Materials Science and Engineering A*[J], 2000, 280: 208
- 15 Gong Ziqi, Chen Ziyong, Chai Lihua et al. *Transactions of Materials and Heat Treatment*[J], 2014, 35: 205 (in Chinese)
- 16 Morisue T, Yajima T, Kume T et al. *IEEE Transactions on Magnetics*[J], 1993, 29: 1562
- 17 Huang A, Loretto M H, Hua D et al. *Intermetallics*[J], 2006, 14: 838
- 18 Mi J, Harding R A, Wickins M et al. *Intermetallics* [J], 2003, 11: 377
- 19 Kong F T, Li B H, Chen Y Y et al. *Journal of Rare Earth*[J], 2004, 22: 150
- 20 Peng K P, Chen W Z, Qian K W. *Key Engineering Materials* [J], 2005, 297: 2508
- 21 Chen Ziyong, Gong Ziqi, Chai Lihua et al. *Materials Science and Technology*[J], 2013, 29: 937
- 22 Gerling R, Leitgeb R, Schimansky F P. *Materials Science and Engineering A*[J], 1998, 252: 23

## 铸造条件对重力铸造 TiAlNb 铸件缩孔及夹杂气泡的影响

宫子琪, 柴丽华, 周峰, 陈子勇, 聂祚仁  
(北京工业大学, 北京 100124)

**摘要:** 研究了感应凝壳炉熔炼的TiAlNb合金的陶瓷型壳重力浇铸。使用了扫描电镜 (SEM), 能谱仪 (EDX) 以及X射线光电子能谱 (XPS) 对铸造合金的显微组织及气孔缺陷进行分析。研究发现, 氧化膜在气孔及缩孔中存在并且是这些缺陷的不均匀形核位置, 而这些气孔缺陷一方面是浇铸过程中气体夹带形成, 另一方面是气体小分子积聚形成。这些气孔广泛存在于铸件的表层及中心部分。铸件直径, 模具温度, 以及氩分压都对气孔缺陷的形成有一定的影响。

**关键词:** 钛铝基合金; 铸造; 微观组织; 缺陷

作者简介: 宫子琪, 男, 1987年生, 博士, 北京工业大学材料科学与工程学院, 北京 100124, 电话: 010-67392280, E-mail: ziqi1029@163.com